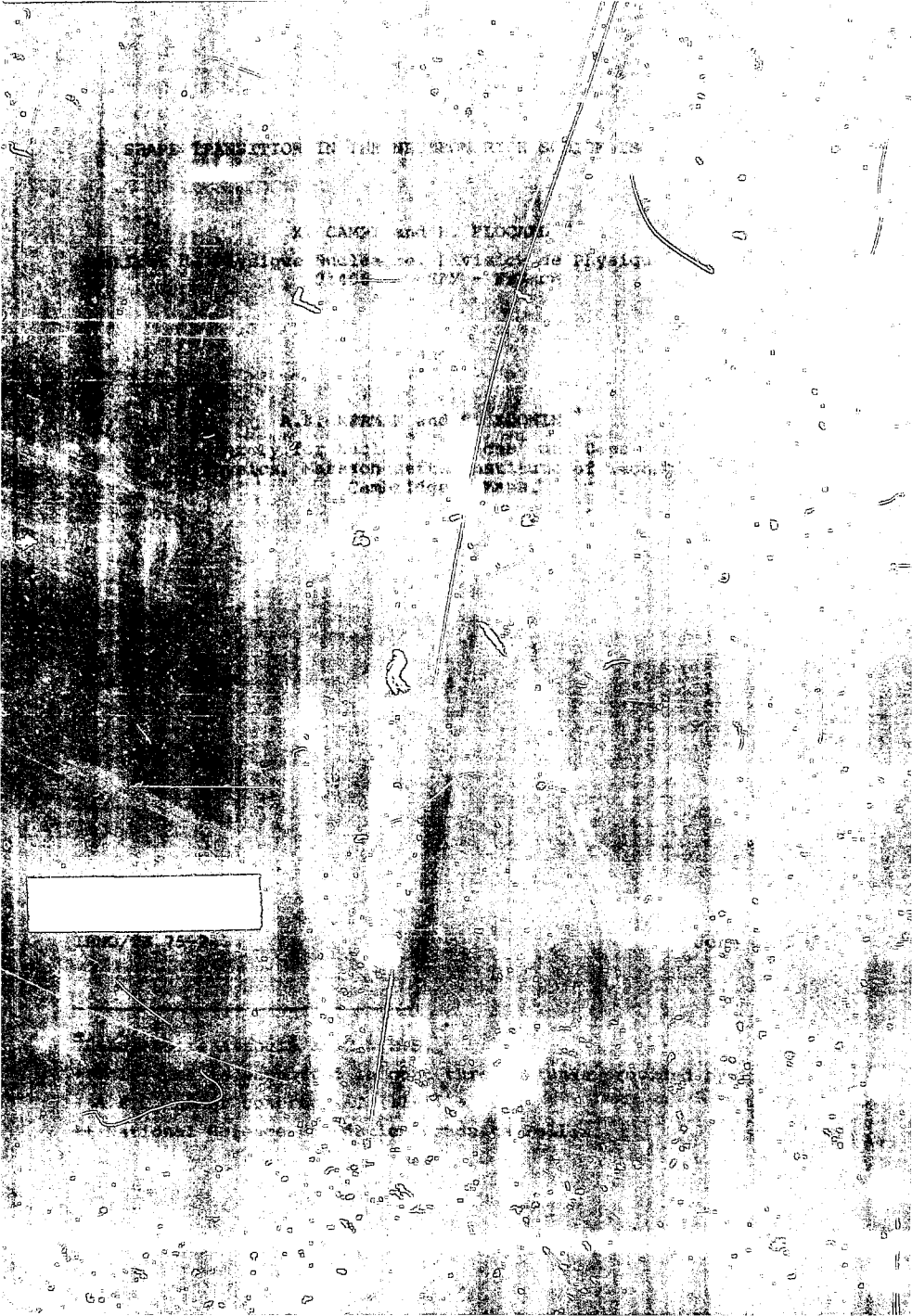

SHAPE TRANSITION IN THE NEUTRON RICH SODIUM ISOTOPES

X. CAMPI and H. FLOCARD

Institut de Physique Nucléaire, Division de Physique Théorique*
91406 - ORSAY - France

and

A.K. KERMAN and S. KOONIN++

Laboratory for Nuclear Sciences+ and Department
of Physics, Massachusetts Institute of Technology
Cambridge - Mass.

IPNO/TH 75-24 - June 1975 -

---

*Laboratoire Associé au C.N.R.S.

+ This work is supported in part through funds provided by the A.E.C. under contract AT (11-1) - 3069

++ National Science Foundation Graduate Fellow.

ABSTRACT

Mass spectrometer measurements of he neutron rich sodium isotopes show a sudden increase at ^{31}Na in the values of the two neutron separation energies. The spherical shell model naturally predicts a sudden decrease at ^{32}Na after the N = 20 shell closure. We propose that the explanation for this disagreement lies in the fact that Sodium isotopes in this mass region are strongly deformed due to the filling of negative parity orbitals from the $1f_{7/2}$ shell. Hartree-Fock calculations are presented in support of this conjecture.

I - INTRODUCTION

Recent experiments performed at C.E.R.N. have measured the total binding energy (B.) of some neutron rich sodium isotopes (1). Consequently the B. systematics are known from ^{19}Na up to ^{32}Na. This corresponds to a variation of the charge asymmetry parameter $\alpha = (N-Z)/A$ ranging from - 0.15 to 0.30. With the exception of He this interval is the largest presently known. The above data therefore provide a check of the symmetry energy in any calculation of the nuclear masses. In addition the two neutron separation energy B_{2n} exhibits a discontinuity at N = 19. A similar effect has long been known for isotopes at N = 88 and is understood in terms of a shape transition from spherical to deformed.

Hartree-Fock (H.F.) and H.F. + B.C.S. calculations performed with the Skyrme interaction have accurately reproduced ground state properties of nuclei from the S-D shell to the actinides (2-5). The deformation energy curves of medium and heavy nuclei (A > 130) (5-7) are in good agreement with those obtained by phenomenological models using the Strutinsky prescription. In addition heavy ion barriers and interaction radii (8,9) are very similar to those of phenomenological potentials adjusted to experimental data. However these calculations have not dealt with nuclei which are very far from the valley of stability. It is therefore of interest to see if the above description can be extended to exotic nuclei like the Na isotopes.

In this paper we present H.F. calculations performed with the Vautherin-Brink version of the Skyrme force (10,11). We have used two of the sets of parameters presented in Ref.12 : SIII and SIV which are shown in Table 1. As discussed in Ref.10, they give very similar predictions for B's, radii and multipole moments of the nuclei lying in the valley of stability. However they have different symmetry energies in nuclear matter : 28 MeV for SIII and 31 MeV for SIV. It is interesting to see if this difference will be reflected in the calculated properties of the exotic Na isotopes.

The following section of this paper presents our method of calculation and discusses the approximations made. The section three discusses the inadequacies of the spherical H.F. approach. The fourth section contains results concerning single particle spectra and deformation energy curves. In section (Va) we discuss binding energies and two neutron separation energies. The properties of the mass and charge densities are given in section (Vb).

II - METHOD OF CALCULATION

The method used to calculate the H.F. ground states is identical to that described and discussed in Refs. (2-4). We recall here some definitions and approximations involved in our calculation.

We impose both axial and reflexion symmetry so that the single particle wave functions can be accurately approximated by a finite expansion in a cylindrical oscillator basis. The basis is defined by two parameters b and q

$$b = \left(\frac{m}{\hbar}\right)^{1/2} (\omega_z\ \omega_\perp^2)^{1/6} \qquad q = \frac{\omega_\perp}{\omega_z} \qquad (1)$$

In formula (1) m is the nucleon mass, ω_z and $\omega_\perp$ are the frequencies along and transverse to the symmetry axis. The parameters b and q we have used for the ground-states are shown in Table 2. The extent of the basis is determined by including all eigenvectors of the oscillator with asymptotic quantum numbers $n_\perp$, n_z and Λ satisfying :

$$\omega_z(n_z+1/2) + \omega_\perp(2n_\perp+|\Lambda|+1) \leq (\omega_z\ \omega_\perp^2)^{1/3}\ (N+2) \qquad (2)$$

The integer N characterizes the size of the basis. For $q \sim 1$ the basis includes the first N+1 oscillator shells. A study of the convergence of binding energies of light nuclei with N has been presented in Ref.2. It was found there that the B. of N=Z nuclei was accurate to better than 400 keV with N = 10. Table 3 shows the B of selected Na isotopes for various values of N. The

conclusions of Ref.2 remain valid even for very neutron rich nuclei.

The method of 2-4 assumes the wave functions to be time-even. For even nuclei this is realized by simultaneously filling time reversal pairs of single particle orbitals. Within the H.F. approximation this is not possible for odd and odd-odd nuclei like the Na isotopes. Therefore for these nuclei we have fixed the occupation probabilities of the last pair of orbitals to be 1/2. This replaces the Slater determinant by a B.C.S. wave function where degenerated orbitals are equally filled*. As discussed in Ref. 13 this approximation will probably lead to small effects on ground state properties. Moreover these effects will be minimized by comparing isotopes differing by two mass units.

The deformation energy curves we present have been obtained by a constrained H.F. calculation as in Refs. (5-9). We use the mass quadrupole moment Q_m as the constraint. It is worthwhile noticing that the empirical formulae of Ref.6 which determine the optimal basis parameters b and q as a function of Q_m are not applicable to such light nuclei. Indeed they assume that the gross properties of the nuclear shape along the deformation path can be correctly approximated by those of a liquid drop. As will be seen in section (Vb), this is not the case for the Na isotopes. Therefore we have determined the optimal values of b and q at each point of the energy curves.

---

*Since only the last orbitals may have non integer occupation probabilities and we introduce no pairing interaction we shall continue to refer to H.F. calculations. This treatment is the natural extension to deformed nuclei of the filling approximation (see e.g. Ref.12). However it should be noted that this way of describing the odd nuclei does not completely eliminate odd-even effects in the binding energies.

III - SPHERICAL H.F. CALCULATIONS

Before discussing the results of our deformed H.F. calculations it is interesting to look at those obtained in calculations where the shape of the nucleus is constrained to be spherical (as in Ref.12,14). In the figure 1 we show the neutron single particle energies obtained with the interactions SIII and SIV for the Na isotopes. As already noted in the case of magic nuclei (12) the level density is higher for SIII than for SIV. This is a consequence of the smaller effective mass of the latter force. We also note that the mean slope of the single particle energies depends strongly on the interaction. While the single neutron energies obtained with SIII are rather constant they decrease with increasing A for SIV. As a result the Fermi energy of any Na isotope is nearly the same for the two interactions despite the different level densities. As the difference between the calculated binding energies of two nuclei is nearly equal to the integral of the calculated Fermi energy. Figure 1 predicts that the variation of B will be about the same for the two forces. This can be seen in Figure 2a which displays the two neutron separation energies versus A. The calculated curve show pronounced structure associated with subshell effects. The mean slope for the two forces are nearly equal implying that the effective symmetry energies for the Na isotopes are about the same. As volume symmetry energies differ (28 MeV for SIII and 31 MeV for SIV) it appears that surface symmetry effects have compensated.

Figure 2a also shows the experimental values of B_{2n}. They are in marked disagreement with the spherical H.F. results. The experimental curve monotonocally decreases from A = 31 to A = 30. In addition it is impossible to correlate the only structure in the experimental data at A = 30, 31 with any of the shell or subshell effects apparent on the spherical H.F.

IV - DEFORMATION ENERGY CURVES

As we have seen the experimental discontinuity in the B_{2n} curve cannot be explained within a spherical H.F. formalism.

A similar feature appears in the rare earth region at N = 88 and is understood in terms of spherical to prolate shape transition. Indeed Nilsson's original level diagram (15) shows the $1/2^-$ and $3/2^-$ states associated with $1f_{7/2}$ crossing $1d_{3/2}$ levels at large prolate deformations. It therefore seems reasonable to investigate wether configurations involving these orbitals might be energetically favoured over the more usual sd shell occupation.

Figure 3 shows the SIII neutron single particle energies for ^{30}Na as functions of the proton quadrupole moment. Apart for an overall scale shift this picture is the same for SIII and SIV and independent of A. For large prolate deformations the $1/2^-$ and $3/2^-$ levels from the $1f_{7/2}$ orbital do cross the $1/2^+$ and $3/2^+$ of $1d_{3/2}$ orbital, so that we are led to consider two different prolate configurations for the sodium isotopes between A = 28 and A = 34. The first is obtained by the usual filling of the $1d_{3/2}$ subshell. The second corresponds to filling the negative parity levels. The analogous level inversion was considered for oblate deformations and the corresponding state found to be highly excited (> 8 MeV) and unstable (particle levels below hole levels). This is largely due to the proton number Z = 11 which favors prolate shapes.

The prolate parts of the deformation energy curves for the isotopes A = 27, 29, 31, 33 and 35 are shown in Fig.4 for the interaction SIII with N = 6 (see Eq.2). Similar results are obtained with SIV. The different segments correspond to various possible occupations. These curves indicate the probability of a transition to a large prolate deformation between A = 31 and A = 32. The competition of this very deformed configuration with the nearly spherical solution is certainly a phenomenon typical of light nuclei. It is not related to the shell effect which explain the fission isomers of the actinide region. In these nuclei the stabilization tends to occur when the shape of the nucleus looks like an ellipsoid with axis ratio $q \sim 2$ (16). Indeed our calculation of ^{240}Pu with SIII (5) gave an optimal value of $q = 1.8$ ($\beta = 0.65$). The second minimum of heavy Na isotopes is not as deformed ($\beta = 0.4$). Its existence strongly depends on the spin-orbit force which brings the $1f_{7/2}$ orbital close to the

$1d_{3/2}$. Furthermore we recognize that the relative importance of each nucleon is large in such light nuclei. Therefore when the proton Fermi level is near a prolate orbital like the $[220]\ 1/2^-$ the last protons can counterbalance the average tendancy against deformation.

V - PROPERTIES OF GROUND-STATE SOLUTIONS

a) Total binding energies : In Table 4 and Figure 5 we present a comparison between the calculated mass defects of the Sodium isotopes and the experimental values. The mean curvature of the data is correctly reproduced by both interactions. This curvature is not solely due to symmetry energy effects because of the changing A along the curve. Since the binding energies calculated with SIII and SIV show similar average behavior with A (12) any difference in the curvature must be due to a difference in symmetry properties. The curvature is smaller with SIV than with SIII implying that the symmetry energy in Sodium nuclei is slightly larger with SIII. This result is opposite to that found in nuclear matter (see introduction) indicating that symmetry energy terms associated with the finite size are very important.

The experimental curve in Figure 5 shows odd-even effects most easily seen in the region $22 < A < 27$. A less pronounced odd-even effect also appears on the calculated curves. But the comparison is not significant because our calculations do not include the proton-neutron pairing effect which may be important in this mass region.

Figure 2b shows the two neutron separation energies. The SIII curve reproduces the data for A between 23 and 30. In contrast the SIV curve exhibits a slope discontinuity at A = 25 which does not appear in data. Furthermore the rotational corrections discussed below accentuate this discrepancy which is due to the low level density. For this reason from now on we shall concentrate on SIII.

The large disagreement that we have at A = 31 can be explained by including rotational zero point energy. This energy is likely to be a smooth function of the deformation and so unimportant for the B_{2n} of most of the isotopes we consider (see quadrupole moments in Table 6). On the other hand ^{19}Na is nearly spherical while ^{21}Na is strongly deformed. This should lead to a significant correction to B_{2n}. The same phenomenon appears again at A = 31.

In order to estimate the magnitude of these corrections we have calculated the rotational energy correction ΔE_k in the following simple approximation 17)

$$\Delta E_k = \frac{\hbar^2}{2\mathcal{J}} \langle J^2 \rangle \qquad (3)$$

where $\mathcal{J}$ is the moment of inertia and $\langle J^2 \rangle$ is the average value of the total angular momentum. In table 5 we give the values $\langle J^2 \rangle$ corresponding to our H.F. solutions. The moments of inertia have been estimated using the rigid body assumption. Because rigid moments are generally larger than experimental values they will result in lower bounds to the rotational energy corrections. In table 6 we see that $\langle J^2 \rangle$ and ΔE_k values grow rapidly at the beginning of the isotope series then decrease slowly from ^{23}Na to ^{31}Na. Here they jump due to the shape transition appears. As can be seen in figure 2c the agreement is noticeably improved (solid line). We have also shown the dotted curve which is obtained assuming that the shape transition occurs at A = 32 as is predicted by the simple H.F. calculations (see chapter IV). As is shown in figure 6 this would require us to take the nearly spherical solution as the ground state of ^{31}Na although it is unfavored by 1.3 MeV after rotational corrections. The same consideration lead us to choose the less deformed solution as the ground state of ^{33}Na.

A measurement of the mass of ^{37}Na would be a very useful check of our picture of Na isotopes since the predictions is that the B_{2n} value is below 5 MeV. In fact we have found that the neutron drip line occurs at ^{37}Na.

b) Nuclear densities and moments : In Table 6 we give the calculated values of the mass and charge quadrupole moments as well as the values of the deformation parameter β_2 of the liquid drop with the same r.m.s. radius and mass quadrupole moment. It is likely that the large deformations in the neutron rich isotopes as large as those found along the valley of stability persist in the neighbouring elements. Calculations to verify this are in progress.

The values of proton (β_{2p}) and mass (β_{2m}) deformation parameters of a given isotope can be very different. This is particularly striking for the isotopes preceding the transition region where the ratio β_{2p}/β_{2m} is close to 1.6. This phenomenon is remarkable since Skyrme H.F. calculation in other regions of the periodic table including such neutron rich nuclei as ^{150}Ce have always led to ratios close to unity. This behavior is probably related to the fact that we have a very large neutron excess in a light nucleus. This result implies that phenomenological calculations should allow for different neutron and proton deformation parameters in this region.

Figure 7 presents two examples of the monopole part of the density distributions (protons and neutrons) calculated using the SIII interaction. The addition of nine neutrons to ^{23}Na produces a sizeable effect on the diffuseness of the proton density because the extra neutrons are largely outside the protons. Of course the small increase in proton deformation parameters between ^{23}Na and ^{32}Na also contributes to the increase of diffuseness.

The only available data is for the nucleus ^{23}Na and has been obtained by both elastic electron scattering 18) and muonic atoms 19). The r.m.s. charge radius is found to be $\langle r_c^2 \rangle^{1/2} = 2.94 \pm 0.06$ fm. Our calculated value (including proton finite size and center of mass corrections) is $\langle r_c^2 \rangle^{1/2} = 3.07$ fm. This result is consistent with the somewhat large radii calculated for other S-D shell nuclei with SIII 2). Since the other Na isotopes are unstable and generally short lived (except for ^{22}Na $T_{1/2} = 2.58$ years) direct measurements of their absolute charge densities will be very difficult. In contrast the isotope shift

$\delta\langle r_c^2\rangle$ can be measured by the doppler-free laser spectroscopy method already employed in the exotic Hg isotopes 20). In figure 8 we have plotted the variation of $\langle r_c^2 \rangle$ (relative to the isotope ^{23}Na) as a function of the mass number A. We also give results of the spherical constrained H.F. calculations (dashed line). This second curve shows practically no structure because of the filling approximation used in the spherical H.F. calculations. The spherical H.F. radii are approximated by an $A^{1/\alpha}$ (α=6) law which is the result of two opposite effects. The addition of neutrons causes the proton orbitals to become more bound thus decreasing the proton radius. On the other hand the strong n-p interaction pulls the proton outwards. The second effect is generally found predominant (see e.g. Ref.21) so that charge radius increases with N. However for neutron deficient Na isotopes the first effect is the more important as the last occupied proton orbital $1d_{5/2}$ becomes nearly unbound. The structure of the solid curve (deformed H.F. calculations) is therefore essentially due to the deformation effects. Comparison of Table 5 and Figure 8 shows a clear correlation between the changes in β_{2p} and the changes in radii. Further experimental work on isotope shifts would therefore provide a good test of the existence of a shape transition at ^{21}Na.

REFERENCES

1) C. Thibault et al. Preprint ORSAY LRB 75-03 to be published in Phys. Rev. C.

2) H. Flocard and P. Quentin, Preprint ORSAY IPNO/TH 75-11

3) H. Flocard, P. Quentin and D. Vautherin, Phys. Lett. 46B (1973) 304

4) M. Brack, P. Quentin and H. Flocard, to be published

5) H. Flocard, P. Quentin, D. Vautherin, M. Véneroni and A.K. Kerman, Nucl. Phys. A231 (1974) 176

6) H. Flocard, P. Quentin, A.K. Kerman and D. Vautherin, Nucl. Phys. A203 (1973) 433

7) M. Cailliau, J. Letessier, H. Flocard and P. Quentin, Phys. Lett. 46B (1973) 11

8) H. Flocard, Phys. Lett. 49B (1974) 129

9) H. Flocard, Communication to the Varenna Summer School July 1974 on "Heavy Ion Reactions"

10) T.H.R. Skyrme, Phil. Mag. 1 (1956) 1043 ; Nucl. Phys. 9 (1959) 615

11) D. Vautherin and D.M. Brink, Phys. Rev. C5 (1972) 626

12) M. Beiner, H. Flocard, Nguyen Van Giai and P. Quentin, Nucl. Phys. A238 (1975) 29

13) A. Faessler, H. Muether and K. Goecke, Z. Phys. 253 (1972) 61

14) M. Beiner, R.J. Lombard and D. Mas, Preprint IPNO/TH 75-4 - ORSAY

15) S.G. Nilsson, Dan. Mat. Fys. Medd. 29 (1955) 16

16) A. Bohr and B. Mottelson, Contribution to the Nobel Symposium 27 Ronneby (1974)

17) W.H. Bassichis, A.K. Kerman and J.P. Svenne, Phys. Rev. 160 (1967) 746

18) G.A. Savitskii et al., Bull. Acad. Sci. USSR Phys. Ser. 33 (1969) 56

19) G.A. Backenstoss et al., Phys. Lett. 25B (1967) 547

20) J. Bonn et al., Phys. Lett. 38B (1972) 308

21) X. Campi, D.W.L. Sprung and J. Martorell, Nucl. Phys. A223 (1974) 541

22) A.H. Wapstra and N.B. Grove, Nucl. Data A9 (1971) 269.

TABLE CAPTIONS

Table 1 : Parameters of the Skyrme irteractions SIII and SIV Notations and units are those of Ref. 11)

Table 2 : Optimal basis parameters used in H.F. calculations of the ground states of sodium isotopes

Table 3 : Convergence of the total binding energies of some sodium isotopes as a function of the size of the basis

Table 4 : Calculated and experimental (1,22) mass defects

Table 5 : Expectation values of the total angular momentum and estimates (see text) of the rotational zero point energy

Table 6 : Mass and charge quadrupole moments in fm^2. The mass and charge deformation parameters are also given.

	t_0	t_1	t_2	t_3	x_0	W
SIII	-1128.75	395.0	-95.0	14000.0	0.45	120.0
SIV	-1205.6	765.0	35.0	5000.0	0.05	150.0

TABLE 1

A	$b_{fm^{-1}}$	q	A	$b_{fm^{-1}}$	q
19	.635	1.28	27	.618	1.23
20	.645	1.3	28	.612	1.19
21	.65	1.37	29	.604	1.16
22	.65	1.37	30	.598	1.09
23	.632	1.34	31	.57	0.98
24	.632	1.27	32	.56	1.32
25	.632	1.2	33	.557	1.34
26	.625	1.2	34	.55	1.24
			35	.55	1.16

TABLE 2

A \ N	4	6	8	10	12
23	-184.651	-184.984	-185.520	-186.631	-186.773
27	-213.923	-214.633	-215.199	-216.462	-216.718
30	-223.179	-224.653	-225.978	-227.073	-227.229

TABLE 3

A	S-III	S-IV	Exp.
19	9.65	10.12	12.98±0.07
20	4.02	6.03	6.84±0.04
21	-2.01	- 0.31	-2.18
22	-5.93	- 3.43	-5.18
23	-9.59	- 7.32	-9.53
24	-9.74	- 6.61	-8.42
25	-10.37	- 7.22	-9.36
26	-8.79	- 5.79	-6.90±0.02
27	-7.13	- 5.09	-5.62±0.06
28	-2.82	- 0.98	-1.14±0.08
29	1.30	2.33	2.65±0.10
30	6.47	6.71	8.37±0.20
31	11.42	10.45	10.60±0.8
32	17.63	16.33	16.4 ±1.1
33	23.20	20.31	-
34	29.82	25.66	-
35	35.70	30.19	-

TABLE 4

A	$\langle J^2 \rangle$	ΔE_{rot}
19	8.29	2.07
20	15.23	3.35
21	18.92	3.78
22	20.04	3.81
23	19.07	3.24
24	18.44	2.95
25	11.43	1.82
26	11.86	1.78
27	12.93	1.81
28	12.84	1.67
29	12.04	1.44
30	10.89	1.31
31	8.07	0.89
32	32.18	3.22
33	33.62	3.02
34	31.47	2.82
35	27.18	2.45

TABLE 5

A	Q_m	β_{2m}	Q_p	β_{2p}
19	33.72	.172	25.80	.212
20	59.68	.276	36.89	.296
21	86.55	.364	46.55	.365
22	93.42	.368	47.28	.369
23	101.14	.373	48.33	.374
24	83.82	.296	40.67	.319
25	64.90	.221	32.63	.259
26	66.86	.213	32.04	.252
27	74.88	.223	33.51	.260
28	69.59	.196	31.42	.242
29	64.30	.170	29.45	.225
30	45.61	.115	22.91	.175
31	148.78	.350	50.56	.390
32	174.12	.367	55.89	.396
33	198.37	.394	60.37	.421
34	177.25	.339	53.90	.376
35	154.77	.286	47.23	.330

TABLE 6

FIGURE CAPTIONS

Figure 1 : Spherical H.F. single particle spectra

Figure 2 : Calculated and experimental two neutron separation energies

Figure 3 : Deformed H.F. single particle spectrum of ^{31}Na

Figure 4 : Prolate parts of deformation energy curves of five Na isotopes

Figure 5 : Experimental and calculated mass defects

Figure 6 : The effect of rotational corrections on the choice of the ground state of ^{31}Na

Figure 7 : Monopole part of proton (dashed line) and neutron (solid line) densities of ^{23}Na and ^{32}Na

Figure 8 : Spherical and deformed H.F. isotope shifts.

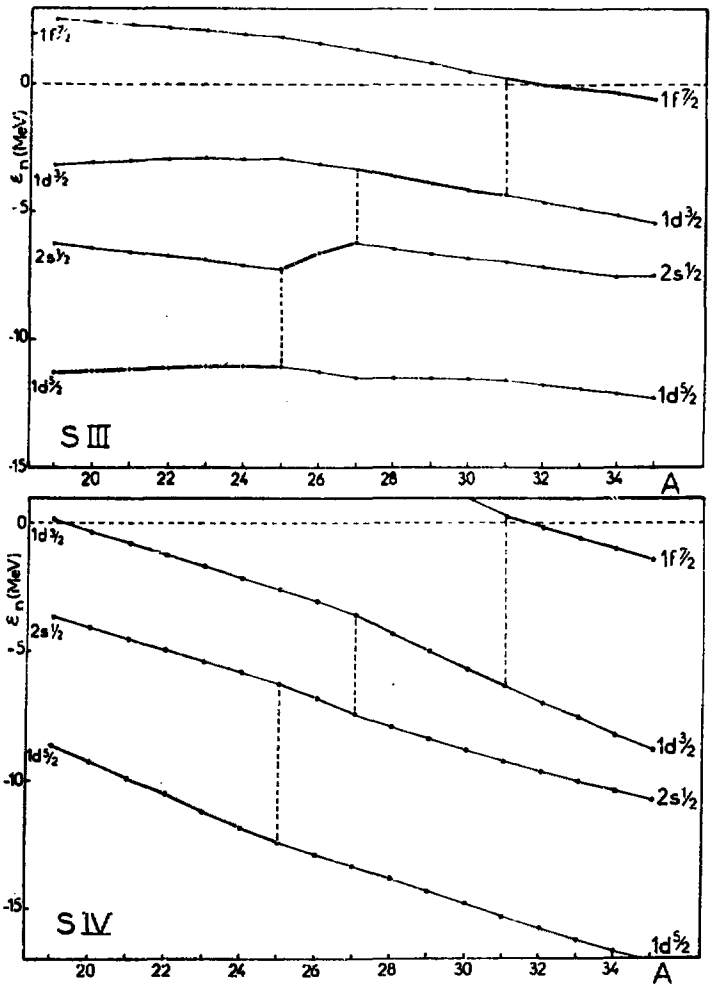
1f7/2
0
1f7/2
εn (MeV)
1d3/2
-5
1d3/2
2s1/2
2s1/2
-10
1d5/2
1d5/2
S III
-15
20
22
24
26
28
30
32
34
A
0
1d3/2
1f7/2
εn (MeV)
2s1/2
-5
1d3/2
1d5/2
2s1/2
-10
S IV
1d5/2
-15
20
22
24
26
28
30
32
34
A

Fig. 1

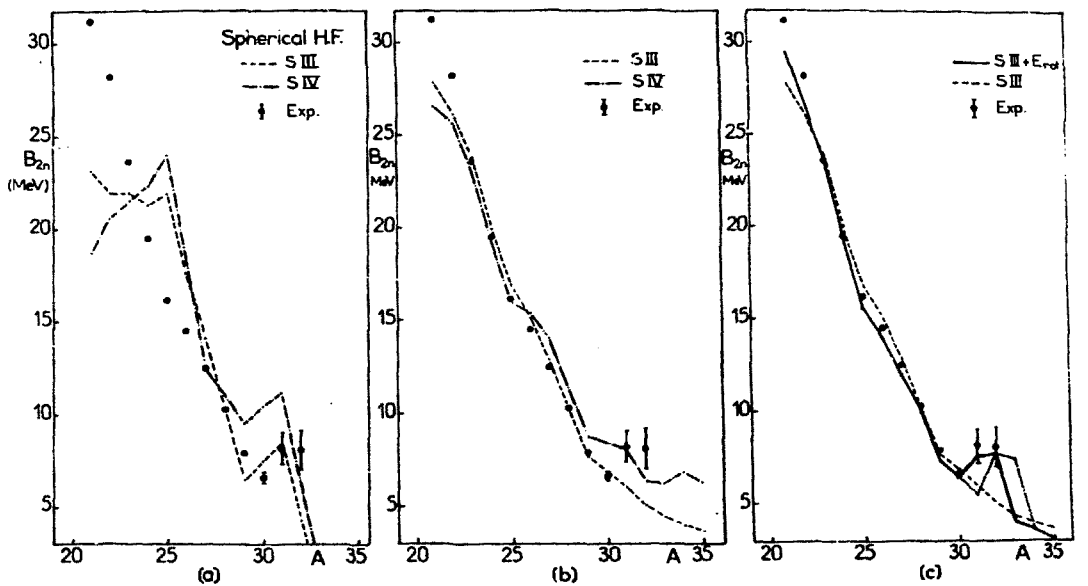
Spherical H.F.
S III
S IV
Exp.
B_{2n} (MeV)
A
(a)
S III
S IV
Exp.
B_{2n} MeV
A
(b)
S III + E_{rot}
S III
Exp.
B_{2n} MeV
A
(c)

Fig. 2

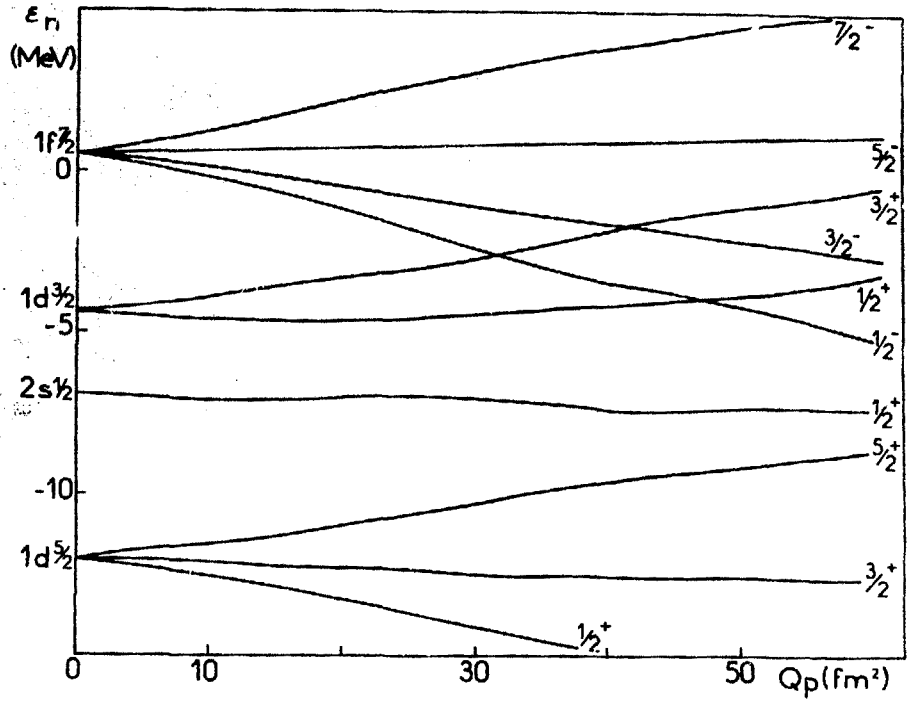
ε_n
(MeV)
1f7/2
0
1d3/2
-5
2s1/2
-10
1d5/2
7/2⁻
5/2⁻
3/2⁺
3/2⁻
1/2⁺
1/2⁻
1/2⁺
5/2⁺
3/2⁺
1/2⁺
0
10
30
50
Qp(fm²)

Fig. 3

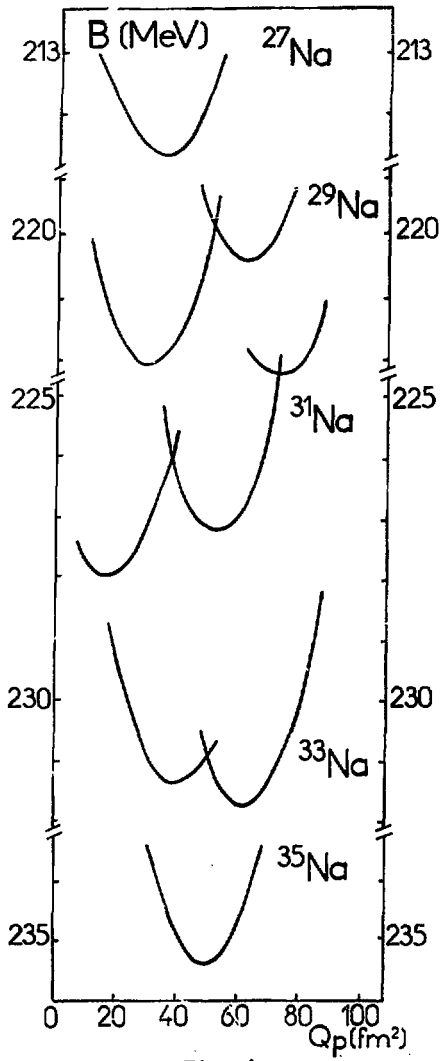
B (MeV)
213
220
225
230
235
^{27}Na
^{29}Na
^{31}Na
^{33}Na
^{35}Na
0
20
40
60
80
100
Qp(fm²)

Fig. 4

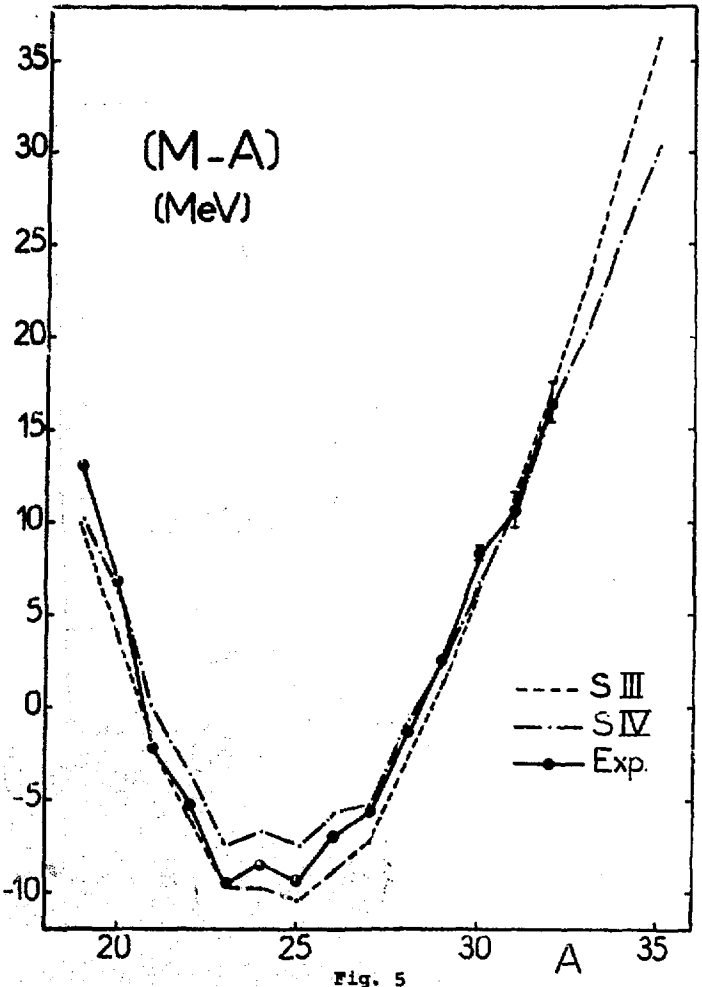

Fig. 5

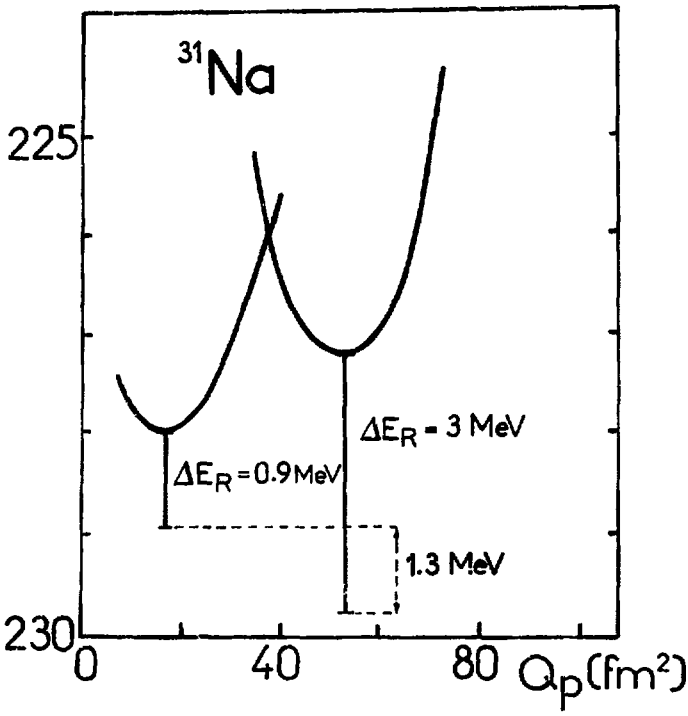

Fig. 6

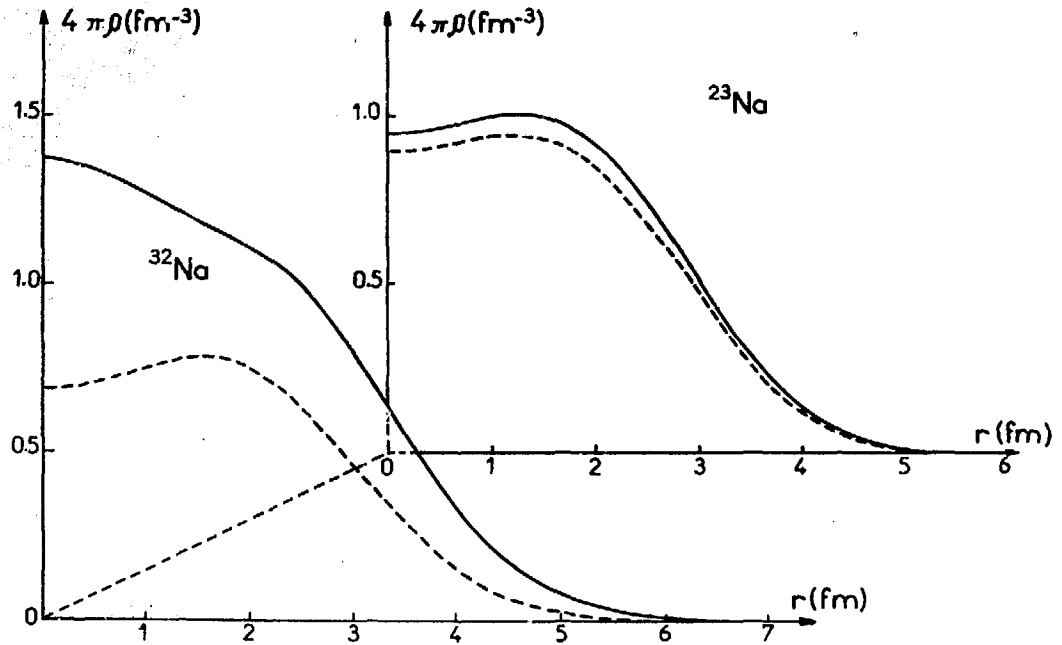
4 πρ(fm⁻³)
1.5
1.0
0.5
0
32Na
1
2
3
4
5
6
7
r(fm)
4 πρ(fm⁻³)
1.0
0.5
23Na
0
1
2
3
4
5
6
r(fm)

Fig. 7

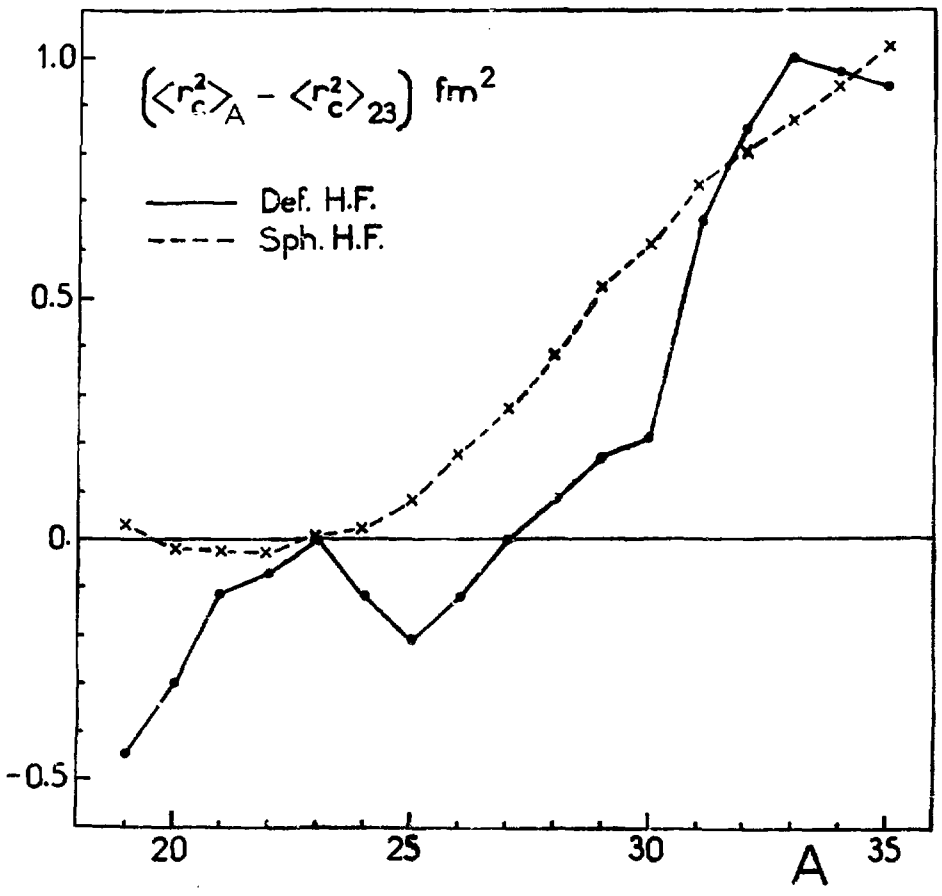
1.0
0.5
0
-0.5
$\left(\langle r_c^2\rangle_A - \langle r_c^2\rangle_{23}\right)$ fm^2
Def. H.F.
Sph. H.F.
20
25
30
35
A

Fig. 8